HOKKAIDO UNIVERSITY

Title	Synthetic Seismograms Near a Finite Fault System
Author(s)	HONDA, Ryou; YOMOGIDA, Kiyoshi
Citation	Journal of the Faculty of Science, Hokkaido University. Series 7, Geophysics, 11(3), 611-632
Issue Date	1999-03-29
Doc URL	http://hdl.handle.net/2115/8852
Type	bulletin (article)
File Information	11(3)_p611-632.pdf

Instructions for use

Synthetic Seismograms Near a Finite Fault System

Ryou Honda and Kiyoshi Yomogida

*Division of Earth and Planetary Sciences, Graduate School of Science,
Hokkaido University, Sapporo 060–0810, Japan*

(Received November 30, 1998)

Abstract

We developed computer codes to synthesize seismograms near a finite fault system with the discrete wave-number method. Besides we synthesized seismograms in two dimensional space, formulations in three dimension are also provided. The discrete wave-number method which regarded circular wave from epicenter as a sum of plane waves propagating any direction is useful in introducing a rectangular fault source and a stratified medium.

1. Introduction

GPS (the Global Positioning System) observation with one–second sampling have been recently able to bear to a practical use. If any analytical method of GPS data is modified suitably, these data can be used as ultra long–period displacement seismograms (Miyazaki et al, 1997). On the other hand, theoretical studies for the solutions of a static deformation of DC component have been also advanced (e.g., Okada, 1985 ; 1992). Inelastic post seismic behavior will be decoupled precisely by proceeding synthetic seismograms with DC component. Additional importance of synthetic seismograms near a finite fault system is the retrieval of detailed fault motions during large earthquakes. Inversions with teleseismic long–period body waves (e.g., Kikuchi and Kanamori, 1996) have been used to reproduce features of fault motions. However, these studies have determined far–field source–time functions and synthesized seismograms to match them with observed waveforms, and they can't sufficiently take into consideration the finiteness of a fault system. Related to high–frequency seismic wave radiation, it is important to obtain relations between rupture propagation and surface displacement. In this study, we formulated seismic waves radiated by a finite fault system in a stratified medium by the discrete wavenumber method of Bouchon and Aki (1972) and Bouchon (1979), with some examples of computations.

2. Potentials due to a point-source

In the Cartesian coordinate system, the displacement vector $\tilde{U}$ can be decomposed into a scaler displacement ϕ and a vector potential $\tilde{\psi}=(\psi_x, \psi_y, \psi_z)$ by

$$\tilde{U} = \nabla\phi + \nabla\times\tilde{\psi}, \quad \nabla\cdot\tilde{\psi} = 0. \tag{1}$$

ϕ and $\tilde{\psi}$ are the solutions of wave equations

$$\nabla^2\phi = \frac{1}{\alpha^2}\frac{\partial^2\psi}{\partial t^2}, \; \nabla^2\tilde{\psi} = \frac{1}{\beta^2}\frac{\partial^2\tilde{\psi}}{\partial t^2}, \tag{2}$$

where α and β are the compressional and shear wave velocities, respectively. When we assume that they have a simple harmonic solution, ϕ and $\tilde{\psi}$ can be written as the following plane waves,

$$\phi = A \exp(ik_x(x-x_o)+ik_y(y-y_o)+i\nu(z-z_o)) \quad z>z_o,$$
$$\phi' = A' \exp(ik_x(x-x_o)+ik_y(y-y_o)-i\nu(z-z_o)) \quad z<z_o,$$
$$\tilde{\psi} = \tilde{B} \exp(ik_x(x-x_o)+ik_y(y-y_o)+i\gamma(z-z_o)) \quad z>z_o,$$
$$\tilde{\psi}' = \tilde{B}' \exp(ik_x(x-x_o)+ik_y(y-y_o)-i\gamma(z-z_o)) \quad z<z_o,$$

where $\nu^2 = k_a^2 - k_x^2 - k_y^2$ ($Im\nu>0$) and $\gamma^2 = k_\beta^2 - k_x^2 - k_y^2$ ($Im\gamma>0$). $k_a = \frac{\omega}{\alpha}$ and $k_\beta = \frac{\omega}{\beta}$ are the wave-numbers for P and S waves respectively and $\omega = \omega_r + i\omega_i$ ($\omega_i>0$) is the angular frequency. Considering boundary conditions at $z=z_o$, coefficients A, A', $\tilde{B}$, and $\tilde{B}'$ are obtained. Since seismic waves decrease as they go away from plane $z=0$ for inhomogeneous waves (i.e., $k_x^2 + k_y^2 > k_a$), $Im\nu$ (imaginary part of ν)>0 so as $Im\gamma>0$. The discrete wave number method used in this study represents seismic waves as the sum of these plane waves. Though such a plane-wave approximation has some disadvantage in terms of the number of integrals, it is useful when we calculate seismic waves radiated from a finite fault and affected by the free surface and horizontal interfaces. The potentials are represented in the form

$$\phi(\tilde{x}, t) = \frac{1}{(2\pi)^3}\int_{-\infty}^{\infty}dk_x\int_{-\infty}^{\infty}dk_y\int_{-\infty}^{\infty}d\omega$$
$$A(k_x, k_y; \omega)\exp(ik_xz(x-x_o)+ik_y(y-y_o)+i\nu|z-z_o|-i\omega t), \tag{3}$$

and $\tilde{\psi}(\tilde{x}, t)$ in a similar manner.

2.1 Single force

We shall first derive the expressions for the displacement potentials radiat-

ed by pulse type point source. We consider the effect of a periodic vertical force of amount $F \exp(ik_x x + ik_y y)$ per unit area acting on the plane $z=0$, which is equivalent to the boundary conditions of traction at $z=0$;

$$\sigma_{zx(z=+0)} = \sigma_{zx(z=-0)},$$
$$\sigma_{zy(z=+0)} = \sigma_{zy(z=-0)},$$
$$\sigma_{zz(z=+0)} + F \exp i(k_x x + k_y y) = \sigma_{zz(z=-0)}.$$

Continuity of displacements at $z=0$ is expressed as

$$\tilde{U}(z=+0) = \tilde{U}(z=-0).$$

Thinking over these boundary conditions and $\nabla \cdot \tilde{\psi} = 0$, we obtain

$$A^z = -A'^z = \frac{F}{2\mu k_\beta^2},$$
$$B_1^z = B_1'^z = \frac{-k_y}{\gamma} A = \frac{-F}{2\mu k_\beta^2} \frac{k_y}{\gamma},$$
$$B_2^z = B_2'^z = \frac{k_x}{\gamma} A = \frac{F}{2\mu k_\beta^2} \frac{k_x}{\gamma},$$
$$B_3^z = B_3'^z = 0.$$

Then, potentials for the vertical single force F are expressed as. follows ;

$$\phi^z = \frac{sgn(z-z_o)F}{8\pi^2\mu k_\beta^2} \int_{-\infty}^{\infty}\int_{-\infty}^{\infty} \exp i(k_x(x-x_o)+k_y(y-y_o)+\nu|z-z_o|)dk_x dk_y,$$
$$\psi_1^z = \frac{-F}{8\pi^2\mu k_\beta^2} \int_{-\infty}^{\infty}\int_{-\infty}^{\infty} \frac{k_y}{\gamma} \exp i(k_x(x-x_o)+k_y(y-y_o)+\gamma|z-z_o|)dk_x dk_y,$$
$$\psi_2^z = \frac{F}{8\pi^2\mu k_\beta^2} \int_{-\infty}^{\infty}\int_{-\infty}^{\infty} \frac{k_x}{\gamma} \exp i(k_x(x-x_o)+k_y(y-y_o)+\gamma|z-z_o|)dk_x dk_y,$$
$$\psi_3^z = 0.$$

Applying this manner to the effect of forces directing in the x or y direction, we also obtain representation of each potentials. Potentials by a force directing in y are

$$\phi^y = \frac{F}{8\pi^2\mu k_\beta^2} \int_{-\infty}^{\infty}\int_{-\infty}^{\infty} \frac{k_y}{\nu} \exp i(k_x(x-x_o)+k_y(y-y_o)+\nu|z-z_o|)dk_x dk_y,$$
$$\psi_1^y = \frac{sgn(z-z_o)}{8\pi^2\mu k_\beta^2} \int_{-\infty}^{\infty}\int_{-\infty}^{\infty} \exp i(k_x(x-x_o)+k_y(y-y_o)+\gamma|z-z_o|)dk_x dk_y,$$
$$\psi_2^y = 0,$$
$$\psi_3^y = \frac{-F}{8\pi^2\mu k_\beta^2} \int_{-\infty}^{\infty}\int_{-\infty}^{\infty} \exp i(k_x(x-x_o)+k_y(y-y_o)+\gamma|z-z_o|)dk_x dk_y,$$

and potentials by a force directing in x are

$$\phi^x = \frac{F}{8\pi^2\mu k_\beta{}^2} \int_{-\infty}^{\infty}\int_{-\infty}^{\infty} \frac{k_y}{\nu} \exp i(k_x(x-x_o)+k_y(y-y_o)+\nu|z-z_o|)dk_xdk_y,$$

$$\psi_1{}^x = 0,$$

$$\psi_2{}^x = \frac{-sgn(z-z_o)F}{8\pi^2\mu k_\beta{}^2} \int_{-\infty}^{\infty}\int_{-\infty}^{\infty}\exp i(k_x(x-x_o)+k_y(y-y_o)+\gamma|z-z_o|)dk_xdk_y,$$

$$\psi_3{}^x = \frac{F}{8\pi^2\mu k_\beta{}^2} \int_{-\infty}^{\infty}\int_{-\infty}^{\infty} \frac{k_y}{\gamma} \exp i(k_x(x-x_o)+k_y(y-y_o)+\gamma|z-z_o|)dk_xdk_y.$$

2.2 Coupled force

Next, we consider displacement potentials radiated from a coupled point source. To do this, we differentiate potentials obtained in the previous section. (See Fig. 1a.). For a double-couple point source (i.e., shear dislocation) located at (x_o, y_o, z_o), the displacement potentials ϕ and ψ can be expressed as functions of the potentials radiated by the point force F with the seismic moment M_o. For instance, considering a right-lateral fault with the strike in the y direction (Fig. 1b), potentials are obtained by

$$\phi = \frac{M_o}{F}\left(\frac{\partial\phi^y}{\partial x_o}+\frac{\partial\phi^x}{\partial y_o}\right),$$

$$\bar{\psi} = \frac{M_o}{F}\left(\frac{\partial\bar{\psi}^y}{\partial x_o}+\frac{\partial\bar{\psi}^x}{\partial y_o}\right).$$

We represent the above force systems as $M_{yx}+M_{xy}$. The general representations of potentials for M_{ij} are as follows;

[Potentials of M_{xx}]

$$\phi = \frac{-M_{xx}}{8\pi^2\mu k_\beta{}^2} \int_{-\infty}^{\infty}\int_{-\infty}^{\infty} \frac{ik_x{}^2}{\nu} \exp i(k_x(x-x_o)+k_y(y-y_o)+\nu|z-z_o|)dk_xdk_y,$$

$$\psi_x = 0,$$

$$\psi_y = \frac{sgn(z-z_o)M_{xx}}{8\pi^2\mu k_\beta{}^2} \int_{-\infty}^{\infty}\int_{-\infty}^{\infty} ik_x \exp i(k_x(x-x_o)+k_y(y-y_o)+\gamma|z-z_o|)dk_xdk_y,$$

$$\psi_z = \frac{-M_{xx}}{8\pi^2\mu k_\beta{}^2} \int_{-\infty}^{\infty}\int_{-\infty}^{\infty} \frac{ik_xk_y}{\gamma} \exp i(k_x(x-x_o)+k_y(y-y_o)+\gamma|z-z_o|)dk_xdk_y.$$

[Potentials of M_{xy}]

$$\phi = \frac{-M_{xy}}{8\pi^2\mu k_\beta{}^2} \int_{-\infty}^{\infty}\int_{-\infty}^{\infty} \frac{ik_xk_y}{\nu} \exp i(k_x(x-x_o)+k_y(y-y_o)+\nu|z-z_o|)dk_xdk_y,$$

$$\psi_x = 0,$$

$$\psi_y = \frac{sgn(z-z_o)M_{xy}}{8\pi^2\mu k_\beta{}^2} \int_{-\infty}^{\infty}\int_{-\infty}^{\infty} ik_y \exp i(k_x(x-x_o)+k_y(y-y_o)+\gamma|z-z_o|)dk_xdk_y,$$

$$\psi_z = \frac{-M_{xx}}{8\pi^2\mu k_\beta{}^2} \int_{-\infty}^{\infty}\int_{-\infty}^{\infty} \frac{ik_xk_y}{\gamma} \exp i(k_x(x-x_o)+k_y(y-y_o)+\gamma|z-z_o|)dk_xdk_y.$$
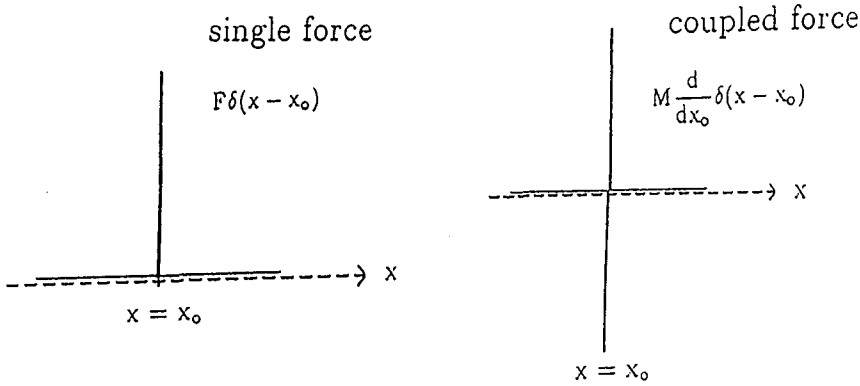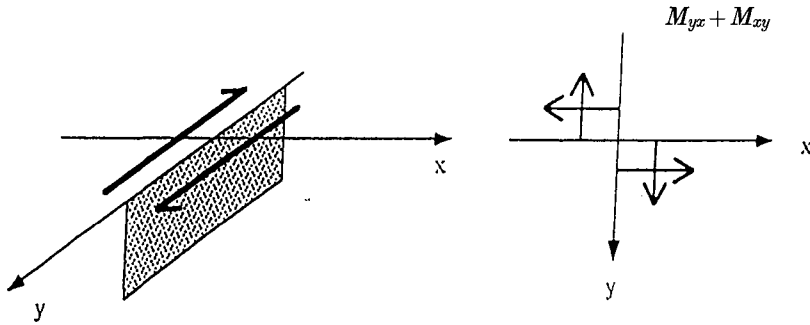
Fig. 1a. Single force and coupled force.

Fig. 1b. Example of a double couple model.

[Potentials of M_{xz}]

$$\phi = \frac{-sgn(z-z_0)M_{xz}}{8\pi^2\mu k_\beta{}^2} \int_{-\infty}^{\infty}\int_{-\infty}^{\infty} ik_x \ \exp \ i(k_x(x-x_o)+k_y(y-y_o)+\nu|z$$
$$-z_0|)dk_xdk_y,$$

$$\psi_x = 0,$$

$$\psi_y = \frac{M_{xz}}{8\pi^2\mu k_\beta{}^2} \int_{-\infty}^{\infty}\int_{-\infty}^{\infty} i\gamma \exp i(k_x(x-x_o)+k_y(y-y_o)+\gamma|z-z_0|)dk_xdk_y,$$

$$\psi_z = \frac{-sgn(z-z_0)M_{xz}}{8\pi^2\mu k_\beta{}^2} \int_{-\infty}^{\infty}\int_{-\infty}^{\infty} ik_y \exp i(k_x(x-x_o)+k_y(y-y_o)$$
$$+ \gamma|z-z_0|)dk_xdk_y.$$

[Potentials of M_{yx}]

$$\phi = \frac{-M_{yx}}{8\pi^2\mu k_\beta{}^2} \int_{-\infty}^{\infty}\int_{-\infty}^{\infty} \frac{ik_xk_y}{\nu} \exp i(k_x(x-x_o)+k_y(y-y_o)+\nu|z-z_0|)dk_xdk_y,$$

$$\psi_x = \frac{-sgn(z-z_o)M_{yx}}{8\pi^2\mu k_\beta{}^2} \int_{-\infty}^{\infty}\int_{-\infty}^{\infty} ik_x \exp i(k_x(x-x_o)+k_y(y-y_o)$$
$$+ \gamma|z-z_o|)dk_x dk_y,$$

$$\psi_y = 0,$$

$$\psi_z = \frac{M_{yx}}{8\pi^2\mu k_\beta{}^2} \int_{-\infty}^{\infty}\int_{-\infty}^{\infty} \frac{ik_x{}^2}{\gamma} \exp i(k_x(x-x_o)+k_y(y-y_o)+\gamma|z-z_o|)dk_x dk_y.$$

[Potentials of M_{yy}]

$$\phi = \frac{-M_{yy}}{8\pi^2\mu k_\beta{}^2} \int_{-\infty}^{\infty}\int_{-\infty}^{\infty} \frac{ik_y{}^2}{\nu} \exp i(k_x(x-x_o)+k_y(y-y_o)+\nu|z-z_o|)dk_x dk_y,$$

$$\psi_x = \frac{-sgn(z-z_o)M_{yy}}{8\pi^2\mu k_\beta{}^2} \int_{-\infty}^{\infty}\int_{-\infty}^{\infty} ik_y \exp i(k_x(x-x_o)+k_y(y-y_o)$$
$$+ \gamma|z-z_o|)dk_x dk_y,$$

$$\psi_y = 0,$$

$$\psi_z = \frac{-M_{yy}}{8\pi^2\mu k_\beta{}^2} \int_{-\infty}^{\infty}\int_{-\infty}^{\infty} \frac{ik_x k_y}{\gamma} \exp i(k_x(x-x_o)+k_y(y-y_o)+\gamma|z-z_o|)dk_x dk_y.$$

[Potentials of M_{yz}]

$$\phi = \frac{-sgn(z-z_o)M_{yz}}{8\pi^2\mu k_\beta{}^2} \int_{-\infty}^{\infty}\int_{-\infty}^{\infty} ik_y \exp i(k_x(x-x_o)+k_y(y-y_o)+\nu|z$$
$$-z_o|)dk_x dk_y,$$

$$\psi_x = \frac{-M_{yz}}{8\pi^2\mu k_\beta{}^2} \int_{-\infty}^{\infty}\int_{-\infty}^{\infty} i\gamma \exp i(k_x(x-x_o)+k_y(y-y_o)+\gamma|z-z_o|)dk_x dk_y,$$

$$\psi_y = 0,$$

$$\psi_z = \frac{sgn(z-z_o)M_{yz}}{8\pi^2\mu k_\beta{}^2} \int_{-\infty}^{\infty}\int_{-\infty}^{\infty} ik_x \exp i(k_x(x-x_o)+k_y(y-y_o)+\gamma|z-z_o|)dk_x dk_y.$$

[Potentials of M_{zy}]

$$\phi = \frac{-sgn(z-z_o)M_{zx}}{8\pi^2\mu k_\beta{}^2} \int_{-\infty}^{\infty}\int_{-\infty}^{\infty} ik_x \exp i(k_x(x-x_o)+k_y(y-y_o)+\nu|z$$
$$-z_o|)dk_x dk_y,$$

$$\psi_x = \frac{M_{zx}}{8\pi^2\mu k_\beta{}^2} \int_{-\infty}^{\infty}\int_{-\infty}^{\infty} \frac{ik_x k_y}{\gamma} \exp i(k_x(x-x_o)+k_y(y-y_o)+\gamma|z-z_o|)dk_x dk_y,$$

$$\psi_y = \frac{-M_{zx}}{8\pi^2\mu k_\beta{}^2} \int_{-\infty}^{\infty}\int_{-\infty}^{\infty} \frac{ik_x{}^2}{\gamma} \exp i(k_x(x-x_o)+k_y(y-y_o)+\gamma|z-z_o|)dk_x dk_y,$$

$$\psi_z = 0.$$

[Potentials of M_{zy}]

$$\phi = \frac{-sgn(z-z_o)M_{zy}}{8\pi^2\mu k_\beta{}^2} \int_{-\infty}^{\infty}\int_{-\infty}^{\infty} ik_y \exp i(k_x(x-x_o)+k_y(y-y_o)+\nu|z$$
$$-z_o|)dk_x dk_y,$$

$$\psi_x = \frac{M_{zy}}{8\pi^2\mu k_\beta{}^2}\int_{-\infty}^{\infty}\int_{-\infty}^{\infty}\frac{ik_x{}^2}{\gamma}\exp\, i(k_x(x-x_o)+k_y(y-y_o)+\gamma|z-z_o|)dk_xdk_y,$$

$$\psi_y = \frac{-M_{zy}}{8\pi^2\mu k_\beta{}^2}\int_{-\infty}^{\infty}\int_{-\infty}^{\infty}\frac{ik_xk_y}{\gamma}\exp\, i(k_x(x-x_o)+k_y(y-y_o)+\gamma|z-z_o|)dk_xdk_y,$$

$$\psi_z = 0.$$

[Potentials of M_{zz}]

$$\phi = \frac{-M_{zz}}{8\pi^2\mu k_\beta{}^2}\int_{-\infty}^{\infty}\int_{-\infty}^{\infty}i\nu\exp\, i(k_x(x-x_o)+k_y(y-y_o)+\nu|z-z_o|)dk_xdk_y,$$

$$\psi_x = \frac{sgn(z-z_o)M_{zz}}{8\pi^2\mu k_\beta{}^2}\int_{-\infty}^{\infty}\int_{-\infty}^{\infty}ik_x\exp\, i(k_x(x-x_o)+k_y(y-y_o)+\gamma|z-z_o|)dk_xdk_y,$$

$$\psi_y = \frac{-sgn(z-z_o)M_{zz}}{8\pi^2\mu k_\beta{}^2}\int_{-\infty}^{\infty}\int_{-\infty}^{\infty}ik_x\exp\, i(k_x(x-x_o)+k_y(y-y_o)$$
$$+\gamma|z-z_o|)dk_xdk_y,$$

$$\psi_y = 0.$$

The moment tensors are related to fault parameters (box 4.4 of Aki and Richards (1980)) by

$$M_{xx} = -M_o(\sin\delta\cos\lambda\sin 2\phi_s+\sin 2\delta\sin\lambda\sin^2\phi_s), \tag{4}$$

$$M_{xy} = M_o(\sin\delta\cos\lambda\cos 2\phi_s+\frac{1}{2}\sin 2\delta\sin\lambda\sin 2\phi_s),$$

$$= M_{yx}, \tag{5}$$

$$M_{xz} = -M_o(\cos\delta\cos\lambda\cos\phi_s+\cos 2\delta\sin\lambda\sin\phi_s), \tag{6}$$

$$= M_{zx},$$

$$M_{yy} = M_o(\sin\delta\cos\lambda\sin 2\phi_s-\sin 2\delta\sin\lambda\cos^2\phi_s), \tag{7}$$

$$M_{yz} - = M_o(\cos\delta\cos\lambda\sin\phi_s-\cos 2\delta\sin\lambda\cos\phi_s), \tag{8}$$

$$= M_{zy},$$

$$M_{zz} = M_o\sin 2\delta\sin\lambda. \tag{9}$$

The seismic moment M_o is given by $M_o=\mu DS$, where μ is the rigidity in the medium, S is the area of the displacement discontinuity and D is the average slip over the fault. The fault geometry is illustrated in Fig. 2. Rupture front propagates in the direction of L with a constant velocity v_r.

3. Potentials due to a finite fault

Next, we integrate potentials for coupled forces distributed along a fault segment to introduce a finite fault source. As shown in Fig. 2, ζ represents the direction of rupture propagating and η is the other direction of the fault segment, with the reference point (x_o, y_o, z_o). Using the transformation of
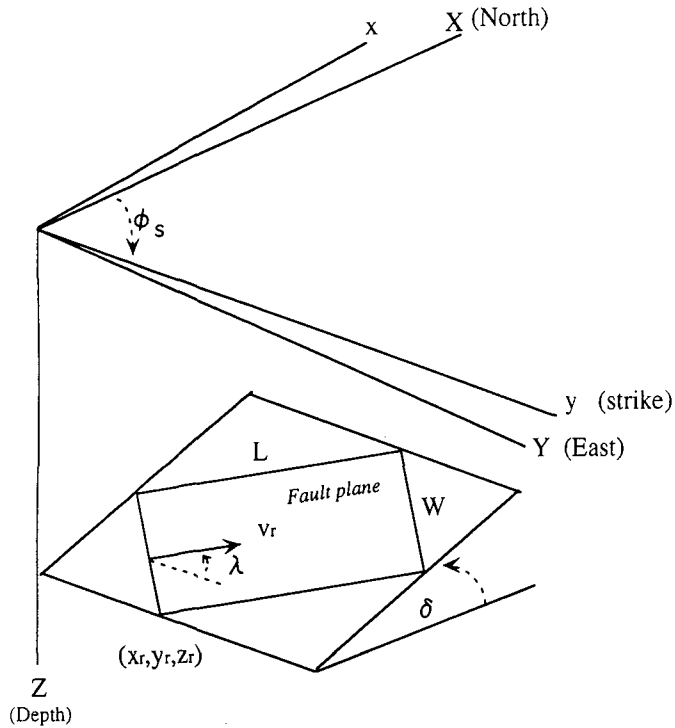
Fig. 2. Geometry of the fault. L, W, ϕ_s, δ and λ are Length, Width, strike, dip and rake of the fault, respectively (after Aki and Richards (1980)).

coordinate

$$
\begin{pmatrix} C_{11} & C_{12} & C_{13} \\ C_{21} & C_{22} & C_{23} \\ C_{31} & C_{32} & C_{33} \end{pmatrix}
$$

$$
= \begin{pmatrix} \sin \phi_s \cos \delta \cos \lambda - \cos \phi_s \sin \lambda & \sin \phi_s \cos \delta \sin \lambda + \cos \phi_s \cos \lambda \\ -\cos \phi_s \cos \delta \cos \lambda - \sin \lambda \sin \phi_s & -\cos \phi_s \cos \delta \sin \lambda + \sin \phi_s \cos \lambda \\ -\sin \delta \cos \lambda & -\sin \delta \lambda \end{pmatrix}
$$

$$
\left. \begin{matrix} \sin \phi_s \sin \delta \\ -\cos \phi_s \sin \delta \\ \cos \delta \end{matrix} \right). \tag{10}
$$

where ϕ_s, λ and δ represent strike, rake and dip, respectively, we can express a posotin on the fault (x_o, y_o, z_o) as

$$\begin{pmatrix} x \\ y \\ z \end{pmatrix} = \begin{pmatrix} C_{11} & C_{12} & C_{13} \\ C_{21} & C_{22} & C_{23} \\ C_{31} & C_{32} & C_{33} \end{pmatrix} \begin{pmatrix} \eta \\ \xi \\ 0 \end{pmatrix} + \begin{pmatrix} x_o \\ y_o \\ z_o \end{pmatrix}.$$

After the above operation, we integrate potentials as follows;

$$\int_o^L \int_o^W \exp i \left(\frac{\omega}{v_r}\xi - k_x(C_{11}\eta + C_{12}\xi) - k_y(C_{21}\eta + C_{22}\xi) \pm \nu(C_{31}\eta + C_{32}\xi) \right) d\eta d\xi.$$

Then we can obtain the expressions of potentials radiated from a finite fault (see Chin (1992)) by

$$\phi_\pm = \frac{iD}{2L_xL_yk_\beta^2} A_\pm \exp i(k_x(x-x_o)+k_y(y-y_o)\mp\nu(z-z_o)),$$

$$\cdot \frac{\{\{\exp iW(-C_{11}k_x-C_{21}k_y\pm C_{31}\nu)-1\}}{(-C_{11}k_x-C_{21}k_y\pm C_{31}\nu)i}$$

$$\cdot \frac{\exp iL(\omega/v_r-C_{12}k_x-C_{22}k_y\pm C_{32}\nu)-1\}}{(\omega/v_r-C_{12}k_x-C_{22}k_y\pm C_{32}\nu)i}$$

$$= C_{P\pm} \exp(\mp i\nu_i z) \tag{11}$$

$$\psi_{SV\pm} = \frac{iD}{2L_xL_yk_\beta^2} B_{sv\pm} \exp i(k_x(x-x_o)+k_y(y-y_o)\mp\gamma(z-z_o)),$$

$$\cdot \frac{\{\exp iW(-C_{11}k_x-C_{21}k_y\pm C_{31}\gamma)-1\}}{(-C_{11}k_x-C_{21}k_y\pm C_{31}\gamma)i}$$

$$\cdot \frac{\{\exp iL(\omega/v_r-C_{12}k_x-C_{22}k_y\pm C_{32}\gamma)-1\}}{(\omega/v_r-C_{12}k_x-C_{22}k_y\pm C_{32}\gamma)i}$$

$$= C_{SV\pm} \exp(\mp i\gamma_i z) \tag{12}$$

$$\psi_{SH\pm} = \frac{iD}{2L_xL_yk_\beta^2} B_{sh\pm} \exp i(k_x(x-x_o)+k_y(y-y_o)\mp\gamma(z-z_o)),$$

$$\cdot \frac{\{\exp iW(-C_{11}k_x-C_{21}k_y\pm C_{31}\gamma)-1\}}{(-C_{11}k_x-C_{21}k_y\pm C_{31}\gamma)i}$$

$$\cdot \frac{\{\exp iL(\omega/v_r-C_{12}k_x-C_{22}k_y\pm C_{32}\gamma)-1\}}{(\omega/v_r-C_{12}k_x-C_{22}k_y\pm C_{32}\gamma)i}$$

$$= C_{SH\pm} \exp(\mp i\gamma_i z) \tag{13}$$

where

$$k_x = \frac{2\pi}{L_x}\cdot n_x, \quad k_y = \frac{2\pi}{L_y}\cdot n_y,$$

$$A_\pm = -\frac{k_x^2}{\nu} M_{xx} - \frac{2k_xk_y}{\nu} M_{xy} \pm 2k_xM_{xz} - \frac{k_y^2}{\nu} M_{yy} \pm 2k_yM_{yz} - \nu M_{zz}, \tag{14}$$

$$B_{sv\pm} = \mp\frac{k_x^2}{k} M_{xx} \mp \frac{2k_xk_y}{k} M_{xy} + \frac{k_x(k_\beta^2-2k^2)}{\gamma k} M_{xz} \mp \frac{k_y^2}{k} M_{yy}$$

$$- \frac{k_y(k_\beta^2-2k^2)}{\gamma k} M_{yz} \pm kM_{zz}, \tag{15}$$

$$B_{sh\pm} = -\frac{k_x k_y}{\gamma} M_{xx} + \frac{k x^2 - k_y^2}{\gamma} M_{xy} \pm k_y M_{xz} + \frac{k_x k_y}{\gamma} M_{yy} \mp k_x M_{yz}, \qquad (16)$$

The plus and minus signs in the above equations correspond to upward and downward propagating potentials, respectively. In the next section, in order to introduce a finite fault buried in a layered medium, we need to consider reflection and transmission coefficients in each layer and at a surface. In such a case, it is reasonable that P-SV and SH motions are separated by making use of the cylindrical symmetry of the medium. For every horizontal wave-number pair (k_x, k_y), let us define a new coordinate system (X', Y', Z') with the X' axis oriented from the source to an observer. In the new coordinate, the horizontal wave-number vector $\tilde{k} = k_x \hat{x} + k_y \hat{y}$, where $\hat{x}$ and $\hat{y}$ are the unit vectors in the x and y directions, respectively (Fig. 3). The displacements in the X and Z directions are for P and SV waves, while in the Y direction for SH wave in the new coordinate. The potentials decoupled into these two kinds of shear waves are then

$$\phi_{SV} = \frac{k_x}{k} \phi_y - \frac{k_y}{k} \phi_x,$$

$$\phi_{SH} = \phi_z,$$

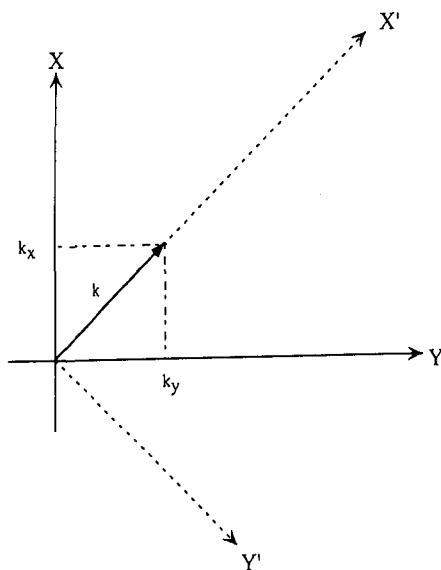where k is the absolute value of horizontal wave-number, that is, $k^2 = k_x^2 + k_y^2$,

Fig. 3. Horizontal wave-number vector Ř, propagating in the X' direction.

and ψ_{SV} and ψ_{SH} represent the SV and SH displacement potentials, respectively.

4. Layered structure

Since the propagator matrix method was introduced in seismology by Haskell (1964), several numerical methods for synthetic seismograms in a layered medium are formulated and developed (e.g., Dunkin, 1965 ; Fuchs, 1968a ; Luco and Apsel, 1983).   In this study, we use the recursive algorithm of generalized transmission and reflection coefficients (called the reflection matrix method) introduced by Kennett and Kerry (1979) in the first, later reformulated by Luco and Apsel (1983).   The relationship between displacement-stress vectors and displacement potentials, $\psi_{\pm}^i$, $\psi_{\pm SV}^i$ and $\psi_{\pm SH}^i$, in the i th layer is given in P-SV case by

$$
\begin{pmatrix} \tilde{U}_i(z) \\ \tilde{\sigma}_i(z) \end{pmatrix} = \begin{pmatrix} I_{11}^i & I_{12}^i \\ I_{21}^i & I_{22}^i \end{pmatrix} \begin{pmatrix} \psi_-^i \\ \psi_{SV-}^i \\ \psi_+^i \\ \psi_{SV+}^i \end{pmatrix},
\tag{17}
$$

$$
\begin{pmatrix} I_{11}^i & I_{12}^i \\ I_{21}^i & I_{22}^i \end{pmatrix} = \begin{pmatrix} ik & -i\gamma_i & ik & i\gamma_i \\ i\nu_i & ik & -i\nu_i & ik \\ -2k\nu_i\mu_i & -l_i\mu_i & 2k\nu_i\nu_i & -l_i\mu_i \\ l_i\mu_i & -2k\gamma_i\mu_i & l_i\mu_i & 2k\gamma_i\mu_i \end{pmatrix},
\tag{18}
$$

where $l_i = (2k^2 - k^2_{\beta i})$ and in SH case,

$$
\begin{pmatrix} \tilde{U}_i(z) \\ \tilde{\sigma}_i(z) \end{pmatrix} = \begin{pmatrix} I_{11}^i & I_{12}^i \\ I_{21}^i & I_{22}^i \end{pmatrix} \begin{pmatrix} \psi_{SH-}^i \\ \psi_{SH+}^i \end{pmatrix},
\tag{19}
$$

$$
\begin{pmatrix} I_{11}^i & I_{12}^i \\ I_{21}^i & I_{22}^i \end{pmatrix} = \begin{pmatrix} ik & ik \\ -\mu_i\gamma_i k & \mu_i\gamma_i k \end{pmatrix}.
\tag{20}
$$

Each displacement potential matrix can be decoupled to the following two parts ;

$$
\begin{pmatrix} \tilde{U}_i(z) \\ \tilde{\sigma}_i(z) \end{pmatrix} = \begin{pmatrix} I_{11}^i & I_{12}^i \\ I_{21}^i & I_{22}^i \end{pmatrix} \begin{pmatrix} E_d^i(z) & 0 \\ 0 & E_u^i(z) \end{pmatrix} \begin{pmatrix} \eta_d^i(z) \\ \eta_u^i(z) \end{pmatrix},
\tag{21}
$$

where $E_d^i(z)$ and $E_u^i(z)$ are, in P-SV case,

$$
E_d^i(z) = \begin{pmatrix} \exp(i\nu_i(z-z_{i-1})) & 0 \\ 0 & \exp(i\gamma_i(z-z_{i-1})) \end{pmatrix},
\tag{22}
$$

$$E_u^i(z) = \begin{pmatrix} \exp(-i\nu_i(z-z_i)) & 0 \\ 0 & \exp(-i\gamma_i(z-z_i)) \end{pmatrix},$$ (23)

and in SH case,

$$E_d^i = \exp(i\gamma_i(z-z_{i-1})), \quad E_u^i = \exp(-i\gamma_i(z-z_{-i})).$$ (24)

Amplitudes of seismic waves radiated from a source are given, in SV case,

$$S_d^l(z) = \begin{pmatrix} C_{P-}\exp(i\nu_l z_{l-1}) \\ C_{Sv-}\exp(i\gamma_l z_{l-1}) \end{pmatrix},$$

$$S_u^l(z) = \begin{pmatrix} C_{P+}\exp(-i\nu_l z_l) \\ C_{Sv+}\exp(-i\gamma_l z_l) \end{pmatrix},$$ (25)

and in SH case,

$$S_d^l(z) = C_{SH-}\exp(i\gamma_l z_{l-1}),$$
$$S_u^l(z) = C_{SH+}\exp(-i\gamma_l z_l). \qquad (z_{l-1} \le z \le z_l),$$ (26)

The coefficients $C_{P\pm}$, $C_{Sv\pm}$ and $C_{SH\pm}$ are the source potentials derived from equations (11)-(16).

4.1 Modified Reflection and Transmission Coefficients

The 2×2 (1×1 in SH case) matrices, R_u^i and R_d^i, represent the modified reflection coefficients for waves incident through the i_th interface from below and above, respectively, as shown in Fig. 4. The terms T_d^i and T_u^i represent the corresponding modified transmission coefficients. The down-going amplitude vector η_d^{i+1} in the $(i+1)$_th layer must be equal to the transmission field $T_d^i \eta_d^i$
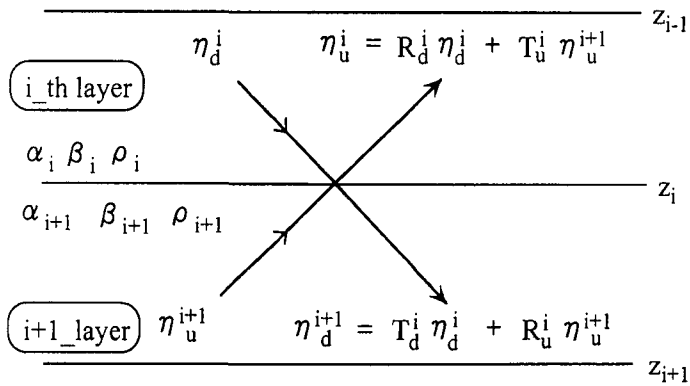

Fig. 4. Modified reflection and transmission coefficients.

from the upper i_th layer plus the reflected field $R_u^i \eta_u^{i+1}$ from the $(i+1)$_th layer, as shown in Fig. 4. So for the up-going wave field η_u^i, as illustrated in Fig. 4. Amplitude vectors are related to reflection and transmission coefficients by

$$\begin{pmatrix} \eta_d^{i+1} \\ \eta_u^i \end{pmatrix} = \begin{pmatrix} T_d^i & R_u^i \\ R_d^i & T_u^i \end{pmatrix} \begin{pmatrix} \eta_d^i \\ \eta_u^{i+1} \end{pmatrix}. \tag{27}$$

From the continuity of both displacement and stress at each boundary, the boundary conditions are given by

$$U_i = U_{i+1}, \quad \text{at } z = z_i,$$

and

$$\sigma_i = \sigma_{i+1}, \quad \text{at } z = z_i,$$

Equation (21) can be expanded as,

$$I_{11}^i E_d^i(z_i)\eta_d^i + I_{12}^1 E_u^i(z_i)\eta_u^i = I_{11}^{i+1}E_d^{i+1}(z_i)\eta_d^{i+1} + I_{12}^{i+1}E_u^i(z_i)\eta_u^{i+1}, \tag{28}$$

$$I_{21}^i E_d^i(z_i)\eta_d^i + I_{22}^i E_u^i(z_i)\eta_u^i = I_{21}^{i+1}E_d^{i+1}(z_i)\eta_d^{i+1} + I_{22}^{i+1}E_u^i(z_i)\eta_u^{i+1}, \tag{29}$$

where $E_u^i(z_i) = E_d^{i+1}(z_i) = I$ and I is the identity matrix. The above expressions can be rewritten as

$$\begin{pmatrix} \eta_d^{i+1} \\ \eta_u^i \end{pmatrix} = \begin{pmatrix} -I_{11}^{i+1} & I_{12}^i \\ -I_{21}^{i+1} & I_{22}^i \end{pmatrix}^{-1} \begin{pmatrix} -I_{11}^i & I_{12}^{i+1} \\ -I_{21}^i & I_{22}^{i+1} \end{pmatrix} \begin{pmatrix} E_d^i(z_i) & 0 \\ 0 & E_u^{i+1}(z_i) \end{pmatrix} \begin{pmatrix} \eta_d^i \\ \eta_u^{i+1} \end{pmatrix}. \tag{30}$$

Comparing equation (27) with equation (30), we obtain the expression for modified coefficient matrices as (defined by Luco and Apsel, 1983):

$$\begin{pmatrix} T_d^i & R_u^i \\ R_d^i & T_u^i \end{pmatrix} = \begin{pmatrix} -I_{11}^{i+1} & I_{12}^i \\ -I_{21}^{i+1} & I_{22}^i \end{pmatrix}^{-1} \begin{pmatrix} -I_{11}^i & I_{12}^{i+1} \\ -I_{21}^i & I_{22}^{i+1} \end{pmatrix} \begin{pmatrix} E_d^i(z_i) & 0 \\ 0 & E_u^{i+1}(z_i) \end{pmatrix}. \tag{31}$$

In the above equations, the modified coefficient matrix is a function of density, P-, S-wave velocities and rigidity, and the matrices $E_d^i(z_i)$ and $E_u^{i+1}(z_i)$ are related to the thicknesses of the i_th and $(i+1)$_th layer, respectively. Therefore, the modified reflection and transmission coefficient matrices can be calculated for a given horizontal wave-number k, at any i_th interfaces, given layer parameters such as α_i, β_i, μ_i and thickness h_i. We derive the reflection coefficient at the free surface. At the free surface, applying the free-stress boundary condition, $\sigma_1(z=0)=0$, we obtain

$$I_{21}^1 E_d^1(z=0)\eta_d^1(0) + I_{22}^1 E_u^1(z=0)\eta_u^1(0) = 0, \tag{32}$$

where $E_d^1(z=0) = I$ and the wave field reflected at the surface is,

$$\eta_d^1 = R_u^0 \eta_u^1(0). \tag{33}$$

Comparing the above expression with equation (32), we obtain the reflection coefficient at the free surface in P-SV case by

$$R_u^0 = -(I_{21}^1)^{-1}I_{22}^1 E_u^1(z=0)$$

$$= \begin{pmatrix} \dfrac{-(2k^2-k_{\beta1}^2)^2+4k^2\gamma_1\nu_1}{F_1}e^{i\nu_1z_1} & \dfrac{4k\gamma_1(2k^2-k_{\beta1}^2)}{F_1}e^{i\gamma_1z_1} \\ \dfrac{-4k\nu_1(2k^2-k_{\beta1}^2)}{F_1}e^{i\nu_1z_1} & \dfrac{-(2k^2-k_{\beta1}^2)^2+4k^2\gamma_1\nu_1}{F_1}e^{i\gamma_1z_1} \end{pmatrix} \quad (34)$$

where $F_1=(2k^2-k_{\beta1}^2)^2+4k^2\gamma_1\nu_1$ is the Rayleigh function in the first layer, and in SH case,

$$R_u^0 = e^{i\gamma_1z_1} \quad (35)$$

4.2 Generalized Reflection and Transmission Coefficients

We denote $\hat{T}_u^i$, the generalized transmission coefficients, from Chin (1992) (same as Luco and Apsel (1983)). Using this coefficient, the total of up-going fields in the i th layer η_u^i equals the transmitted field from the $(i+1)$ th layer denoted by $\hat{T}_u^i\eta_u^{i+1}$. The physical interpretation of the generalized reflection and transmission coefficients is illustrated in Fig. 5. Down-going wave field η_d^i in this medium can be obtained by multiplying η_u^i by $\hat{R}_u^{i-1}$. $\hat{R}_u^{i-1}$ represents the generalized reflection coefficient in the $(i-1)$ th interface as follows,

$$\begin{aligned}\eta_u^i &= \hat{T}_u^i\eta_u^{i+1} = \hat{T}_u^{i+1}\ldots\hat{T}_u^{l-1}\eta_u^l(z_{l-1}), \\ \eta_d^i &= \hat{R}_u^{i-1}\eta_u^i = \hat{R}_u^{i-1}\hat{T}_u^i\hat{T}_u^{i+1}\ldots\hat{T}_u^{l-1}\eta_u^l(z_{l-1}) \quad (i=1,2,\ldots,l-1).\end{aligned} \quad (36)$$

From equations (27) and (36), we obtain the following recurrence relations:

$$\begin{aligned}\hat{T}_u^i &= (I-R_d^i\hat{R}_u^{i-1})^{-1}T_u^i, \\ \hat{R}_u^i &= R_u^i+T_d^i\hat{R}_u^{i-1}\hat{T}_u^i \quad (i=1,2,\ldots,l-1).\end{aligned} \quad (37)$$

Similarly, for layers below the source,

$$\begin{aligned}\eta_d^i &= \hat{T}_d^{i-1}\eta_d^{i-1} = \hat{T}_d^{i-1}\hat{T}_d^{i-2}\ldots\hat{T}_d^l\eta_d^l(z_l), \\ \eta_u^i &= \hat{R}_d^i\eta_d^i = \hat{R}_d^i\hat{T}_d^{i-1}\hat{T}_d^{i-2}\ldots\hat{T}_d^l\eta_d^l(z_l) \quad (i=N+1,\ldots,l+1),\end{aligned} \quad (38)$$

where N indicates the total number of layers above the half-space. Therefore, once the downwardly amplitude vector $\eta_d^l(z_l)$ at the source layer is determined, then after the sequential multiplication of transmission coefficients $\hat{T}_d^i$, we can obtain the amplitude vector η_u^i and η_d^i in the i th medium by

$$\begin{aligned}\hat{T}_d^i &= (I-R_u^i\hat{R}_d^{i+1})^{-1}T_d^i, \\ \hat{R}_d^i &= R_d^i+T_u^i\hat{R}_d^{i+1}\hat{T}_d^i \quad (i=N,\ldots,l).\end{aligned} \quad (39)$$

Recurring the calculation of equation (37) from the first layer $(i=1)$ to the $(l-1)$ th layer, we can obtain generalized reflection and transmission coefficients in
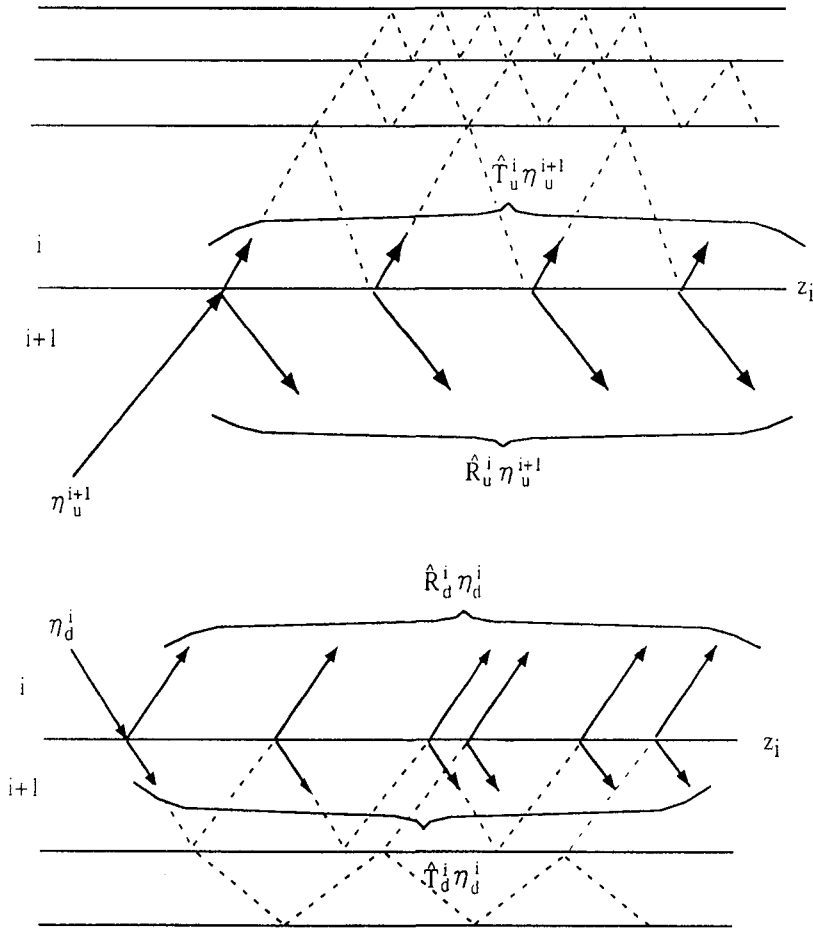
Fig. 5. Interpretation of the generalized reflection and transmission coefficients (reproduced from Chin, (1992)).

each layer above the source. Similarly, $\hat{R}_d^i$ $(i=N+1,\ldots,l)$ can be obtained through the recursive procedure (39). Both $\eta_u^l(z_{l-1})$ and $\eta_d^l(z_l)$ can be derived from the wave field in the source layer. In the medium containing the source $(i=l)$, the upwardly fields $\eta_u^l(z_{l-1})$ can be separated into three terms, namely, the up-going source wave fields $S_u^l(z_{l-1})$, the down-going source fields $\hat{R}_d^l S_d^l(z_l)$ reflected at the lower interface z_l, and $\hat{R}_d^l \eta_d^l(z_{l-1})$. There is reflected down-going wave field $\eta_d^l = \hat{R}_u^{l-1} \eta_u^{l-1}(z_{l-1})$ at z_l. Thus

$$\eta_u^l(z_{l-1}) = S_u^l(z_{l-1}) + \hat{R}_d^l S_d^l(z_l) + \hat{R}_d^l \hat{R}_u^{l-1} \eta_u^l(z_{l-1}),$$

Similarly, $\eta_d^l(z_l)$ is expressed by

$$\eta_d^l(z_l) = S_u^l(z_l) + \hat{R}_u^{l-1} S_u^l(z_{l-1}) + \hat{R}_d^{l-1} \hat{R}_d^l \eta_d^l(z_l).$$

Finally, the above equations become

$$\eta_u^l(z_{l-1}) = (I - \hat{R}_d^l \hat{R}_u^{l-1})^{-1} [S_u^l(z_{l-1}) + \hat{R}_d^l S_d^l(z_l)],$$ (40)

$$\eta_d^l(z_l) = (I - \hat{R}_u^{l-1} \hat{R}_d^l)^{-1} [S_d^l(z_l) + \hat{R}_u^{l-1} S_u^l(z_{l-1})],$$ (41)

where the source terms $S_d^l(z_l)$ and $S_u^l(z_{l-1})$ have been derived in equations (25) and (26). The displacement and stress vectors in the i_th medium can be calculated by expanding equation (21) as

$$\begin{pmatrix} U_i(z) \\ \sigma_i(z) \end{pmatrix} = \begin{pmatrix} I_{11}^i E_d^i(z) \eta_d^i(z) + I_{12}^i E_u^i(z) \eta_u^i(z) \\ I_{21}^i E_d^i(z) \eta_d^i(z) + I_{22}^i E_u^i(z) \eta_u^i(z) \end{pmatrix}$$ (42)

The surface displacements in P-SV case are given by

$$\begin{pmatrix} U(z=0) \\ W(z=0) \end{pmatrix} = I_{11}^1 E_d^1(z=0) \eta_d^1(z=0) + I_{12}^1 E_u^1(z=0) \eta_u^1$$

$$= \begin{pmatrix} ik & -i\gamma_1 \\ i\nu & ik \end{pmatrix} \begin{pmatrix} 1 & 0 \\ 0 & 1 \end{pmatrix} \eta_d^1$$ (43)

$$+ \begin{pmatrix} ik & i\nu_1 \\ -i\nu_1 & ik \end{pmatrix} \begin{pmatrix} \exp(i\nu_1 z_1) & 0 \\ 0 & \exp(i\gamma_1 z_1) \end{pmatrix} \eta_u^1,$$

and in SH case

$$V(z=0) = I_{11}^1 E_d^i(z=0) \eta_d^1 + I_{11}^1 E_u^i(z=0) \eta_u^1$$ (44)

$$= (ik) \eta_d^1 + (ik) \exp(i\gamma_1 z_1) \eta_u^1.$$

All the calculations in this section are done in frequency domain. Time-domain solutions are obtained by the fast Fourier transformation after obtaining solutions in frequency domain.

5. Synthetic Seismograms

Employing the scheme explained in the previous section, we compare our results with those published in previous studies in order to confirm the accuracy of our computer codes.

5.1 Two-Dimensional Half-space

First, we calculate synthetic seismograms with a two dimensional model, radiated from a single line fault whose configuration given in Fig. 6a. The slip time function is a step function. The rupture starts in the bottom of the fault with rupture velocity of 2 km/s and compressional and shear wave velocities of
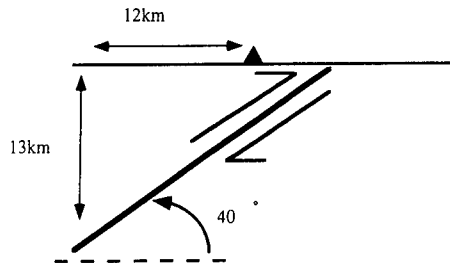
12km

13km

40°

Fig. 6a.   One dimensional fault source.
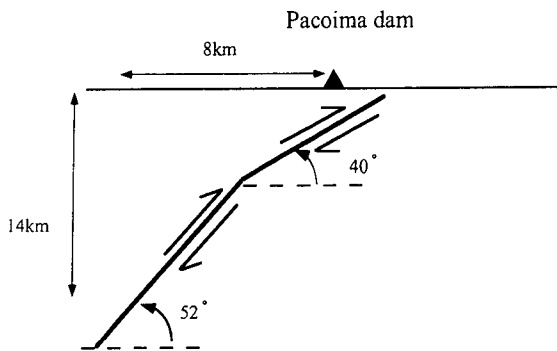
Pacoima dam

8km

40°

14km

52°

Fig. 6b.   Fault plane geometry used for the San Fernando earthquake, with two fault planes.

the medium are 5.6 km/s and 3.2 km/s, respectively.   Computed seismograms are shown in Fig. 7.   Two pulses radiated from the points of rupture nucleation and rupture termination at both ends of the fault are observed.   SP indicates an evanescent P wave propagating along the free surface (Lay and Wallace, 1995). The SP wave have been studied in detail in some papers (e.g., Pekeris and Lifson, 1957 ; Bouchon, 1978).   Our results show good agreement with those of Bouchon (1979).   Next, we try to reproduce the exact solution of Niazy (1973) which represents the record at Pacoima dam during the 1972 San Fernando, California, earthquake.   A considered model is illustrated in Fig. 6b.   A rupture initiates in the bottom of the fault with constant velocities 2.5 km/s and 1.5 km/ s on the lower and the upper segments of the fault.   P and S wave velocities are same as those in the previous example.   A numerical solution solved by Bouchon and Aki (1977) is shown at the lower part of Fig. 8, while our results are shown at the upper part.   In addition to the starting and stopping phases, waves propagate from the break point in the middle of two segments are recognized.
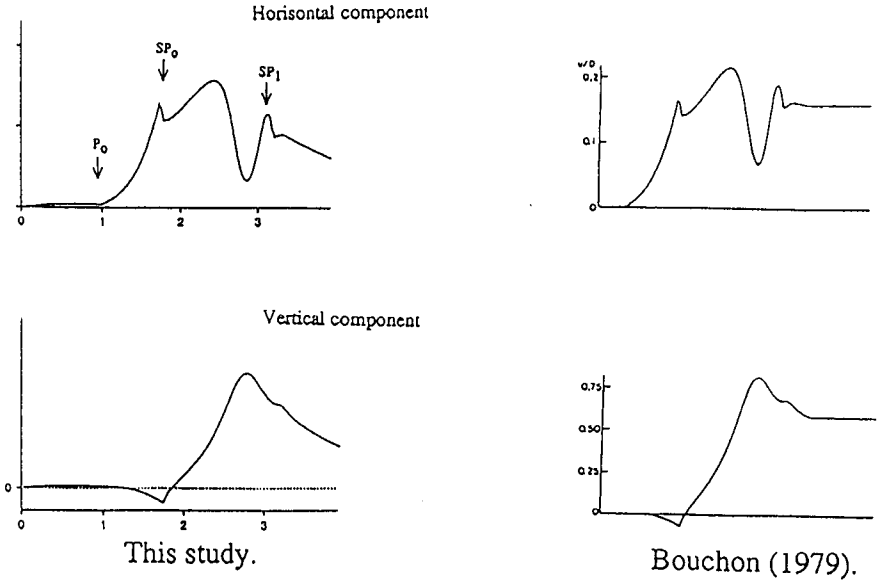
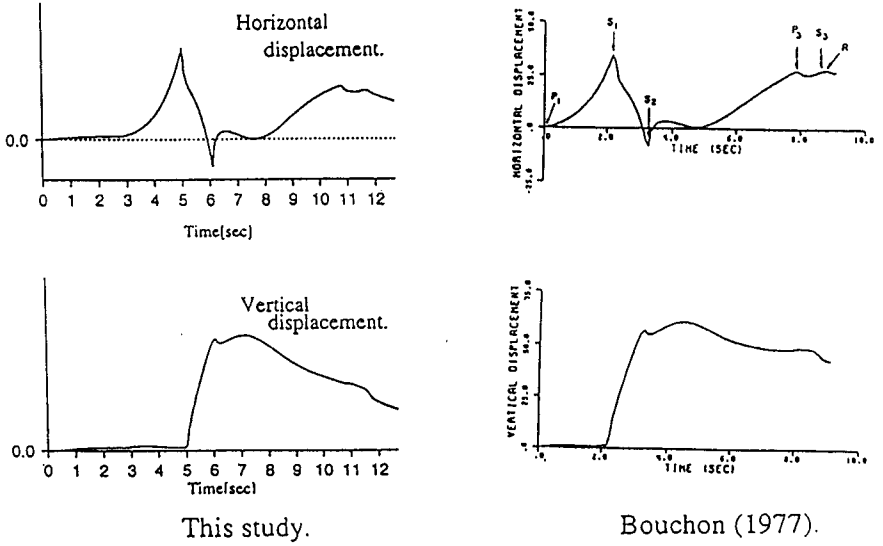Fig. 7.   Synthetic seismograms of one dimensional fault source.

Fig. 8.   Synthetic seismograms of model configured in Fig. 6b.

Fig. 8 also shows good agreement again between our results and Bouchon's. The single difference between our results and Bouchon's is static of DC component. This corresponds to the zero frequency. The choice of the artificial imaginary part of the angular frequency ω_i for the stability of computations may be affected because we must apply the filter of $\exp(-\omega_i t)$ in the final process of calculation of time-domain seismograms. The effect of ω_i as well as other parameters such as δk should be studied in detail to obtain accurate static deformations in further studies.

5.2 Two-Dimensional Layered Medium

We use the reflection matrix method, introduced by Kennett and Kerry (1979), to calculate wave field in a layered medium. As expressed by equations (17) and (19) and shown in Fig. 3, potentials propagating in a layered medium are calculated in a new coordinate (X', Y', Z). We can therefore use the same sub-routine for a 3-D case if calculations in 2-D are successful. To check the accuracy of our sub-routine which includes the effect of a layered medium, we assume a point source buried in a layered medium. The model configuration is shown in Fig. 9. P- and S-wave velocities are 6.0 km/s and 3.5 km/s in the upper medium, and are 8.2 km/s and 4.7 km/s in the lower, respectively. Synthetic seismograms are shown in Fig. 10. We can recognize P and S waves which arrive from the source to the observer directly, followed by phases of P and S waves reflected multiply at the free surface and/or the interface of the two layers. Travel times of these phases can be explained by those estimated by geometrical ray theory, as shown by red and blue broken lines in Fig. 10. It is clear that the interaction of a simple surface layer in this example produces extreme complexity in seismograms.
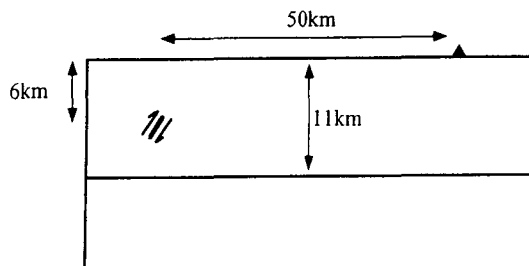

Fig. 9. A point source buried in layered medium. Density of each medium are 2.8 g/cm³ and 3.3 g/cm³, respectively. The dip angle is 45 degree.
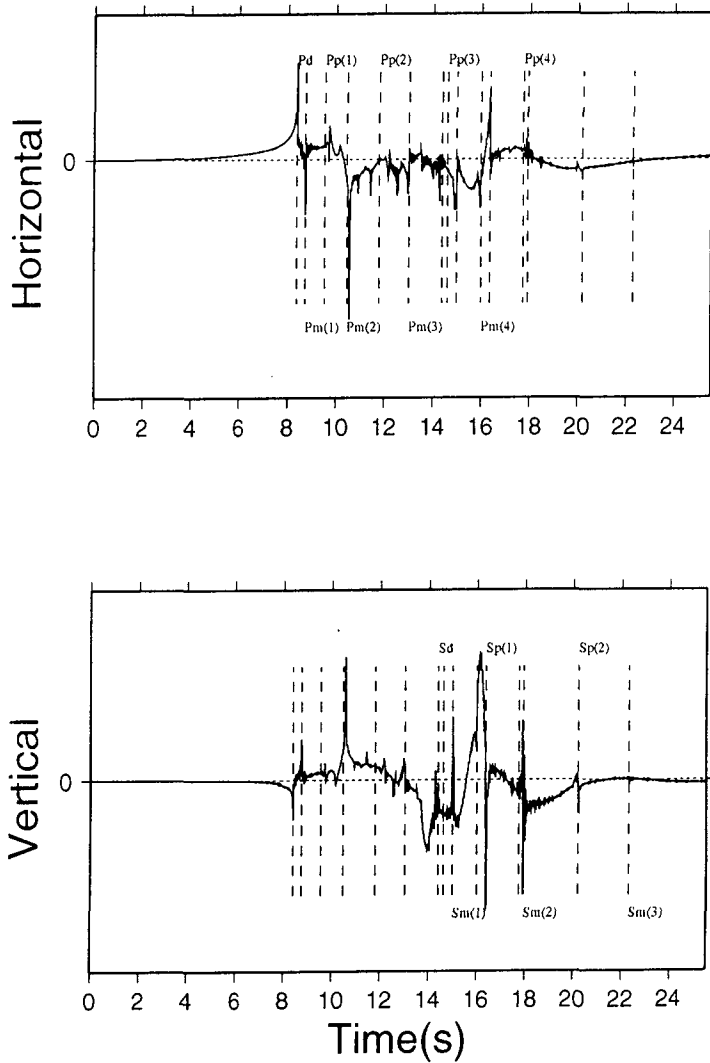
Fig. 10.   Synthetic seismograms due to the model illustrated in Fig. 9.   *Pd* and *Sd*
    indicate direct *P* and *S* waves.   Subscripts *p* and *m* show that waves were
    reflected at upper or lower surface at first, and numbers show how many times
    reflected that waves were.

6.   Conclusions

We synthesized seismograms in 2-D homogeneous isotropic half-space and
a layered medium and results have good agreement with those of other

researches such as Bouchon (1979) and Chin (1992). But we found a little difference of static components. Synthetic seismograms radiated from a point dislocation source in a layered medium show direct P and S waves followed by multiply reflected P and S waves. As the next step, we must study in detail about parameters which relate to static components such as L_x, L_y and Δk in order to estimate static deformation accurately. In addition, we develop 3-D computer codes to calculate more realistic seismograms near a finite fault system.

References

Aki, K. and P.G. Richards, 1980. Quantitative Seismology: Theory and Methods, W.H. Freeman and Co., San Francisco.

Okada, Y., 1985. Surface Deformation due to Shear and Tensile Faults in a Half Space, Bull. Seism. Soc. Am., **75**, 1135-1154.

Bouchon, M., 1977. Discrete Wave number Representation of Seismic source Wave Fields, Bull. Seism. Soc. Am., **67**, 259-277.

Bouchon, M., 1978. A Dynamic Source Model for The San Fernando Earthquake, Bull. Seism. Soc. Am. **68**, 1555-1576.

Bouchon, M., 1978. The Importance of The Surface of Interface P Wave in Near-earthquake Studies, Bull. Seism. Soc. Am., **68**, 1293-1311.

Bouchon, M., 1979. Discrete Wave Number Representation of Elastic Wave Fields in Three-Space Dimensions, J. Geophys. Res., **84**, 3609-3614.

Bouchon, M., 1981. A Simple Method to Calculate Green's Function for Elastic Layered media, Bull. Seism. Soc. Am., **71**, 959-971.

Chin, B.H., 1992. Simultaneous Study of The Source, Path and Site Effects on Strong Ground Motion During The 1989 Loma Prieta Earthquake, Ph. D. Thesis, University of Southern California, pp 196.

Dunkin, J.W., 1965. Computation of modal solutions in layered, elastic media at high frequencies, Bull. Seismol. Soc. Am., **55**, 335-358.

Fuchs, K., 1968a. Das Reflexions- und Transmissionsvermögen eines geschichteten Mediums mit beliebiger Tiefen-Verteilung der elastischen Moduln und der Dichte für schraägen Einfall ebener Wellen, Z. Geophys., **34**, 389-413.

Haskell, N.A., 1964. Total energy and energy spectral density of elastic wave radiation from propagation faults, Bull. Seismol. Soc. Am., **54**, 1811-1814.

Kennett, B.L.N, and N.J. Kerry, 1979. Seismic waves in a stratified half space, Geophys. J. R. astr. Soc., **57**, 557-583.

Kikuchi, M. and H. Kanamori, Inversion of complex body waves, Bull. Seismol. Soc. Am., **72**, 491-509, 1982.

Kikuchi, M. and H. Kanamori, 1986. Inversion of complex body waves-II, Phys. Earth Planet. Interiors, **43**, 205-222.

Lay, T and T.C. Wallace, 1995. Modern Global Seismology, Academic Press, Inc.

Luco, J.E. and R.J. Apsel, 1983. On the Green's functions for layered half-space. Part I, Bull. Seismol. Soc. Am., **73**, 909-929.

Pekeris, C.I., and H. Lifson, 1957. Motion of the surface of a uniform elastic half-pace by a buried pulse, J. Acoust. Soc. Am., **29**, 1233-1238.

Miyazaki, S. Sagiya, T. and Tada, T., 1997. Detection of Seismic Displacement by analyzing

one second GPS data (case of Hyuga earthquake on Dec. 3, 1996).   Abstract of The
Seismological Society of Japan, B04.
Niazy, A., 1973.   Elastic Displacements caused by a propagating crack in an infinite medium :
an exact solution., Bull. Seism. Soc. Am. **63**, 357-379.